

See discussions, stats, and author profiles for this publication at: <https://www.researchgate.net/publication/46035951>

Upgrading of crude algal bio-oil in supercritical water

ARTICLE *in* BIORESOURCE TECHNOLOGY · JANUARY 2011

Impact Factor: 4.49 · DOI: 10.1016/j.biortech.2010.08.013 · Source: PubMed

CITATIONS

81

READS

293

2 AUTHORS:



Peigao Duan

Henan Polytechnic University

44 PUBLICATIONS 961 CITATIONS

SEE PROFILE



Phillip E. Savage

University of Michigan

197 PUBLICATIONS 7,586 CITATIONS

SEE PROFILE

Hydrothermal Liquefaction and Gasification of *Nannochloropsis* sp.

Tylisha M. Brown, Peigao Duan, and Phillip E. Savage*

Department of Chemical Engineering, University of Michigan, Ann Arbor, Michigan 48109-2136

Received February 22, 2010. Revised Manuscript Received April 16, 2010

We converted the marine microalga *Nannochloropsis* sp. into a crude bio-oil product and a gaseous product via hydrothermal processing from 200 to 500 °C and a batch holding time of 60 min. A moderate temperature of 350 °C led to the highest bio-oil yield of 43 wt %. We estimate the heating value of the bio-oil to be about 39 MJ kg⁻¹, which is comparable to that of a petroleum crude oil. The H/C and O/C ratios for the bio-oil decreased from 1.73 and 0.12, respectively, for the 200 °C product to 1.04 and 0.05, respectively, for the 500 °C product. Major bio-oil constituents include phenol and its alkylated derivatives, heterocyclic N-containing compounds, long-chain fatty acids, alkanes and alkenes, and derivatives of phytol and cholesterol. CO₂ was always the most abundant gas product. H₂ was the second most abundant gas at all temperatures other than 500 °C, where its yield was surpassed by that of CH₄. The activation energies for gas formation suggest the presence of gas-forming reactions other than steam reforming. Nearly 80% of the carbon and up to 90% of the chemical energy originally present in the microalga can be recovered as either bio-oil or gas products.

Introduction

Microalgae are versatile biological factories and offer several advantages relative to terrestrial lignocellulosic biomass for renewable biofuel production.^{1,2} Microalgae have a higher photosynthetic efficiency. They can also be rich in oil (triglycerides), harvested frequently because of their rapid growth rate, cultivated in variable climates and on marginal and non-arable land, and grown in both brackish and contaminated water environments. As a result, land requirements are lower and the environmental issues related to global changes in land-use patterns are less problematic for algae cultivation.³ Microalgae can also remove nitrogen, phosphorus, and heavy metals from wastewaters and use N and P as nutrients. Thus, algae cultivation can be coupled with wastewater bioremediation. Furthermore, microalgae cultivation facilities can be integrated with fossil-fuel-fired power plants to recycle CO₂, via photosynthesis, from the flue gas into algal biomass.

The conventional approach for making biofuel from microalgae involves the extraction of triglycerides from the algal biomass and its subsequent conversion (e.g., via transesterification) into biodiesel fuel. This approach requires dewatering of the microalgae, drying of the dewatered biomass paste, and then solvent extraction of the triglycerides from the dried biomass. These steps are costly and require the use of an organic solvent. An alternate approach that requires no drying and no organic solvents is hydrothermal processing. This approach converts the microalgae, with a high moisture content, in water at elevated temperatures and pressures.

Under these conditions, the biomacromolecules in the microalgae break down to form a bio-oil and gases.

The literature provides previous reports of microalgae processing under hydrothermal conditions. Liquefaction studies^{4–10} typically used temperatures between 200 and 350 °C and reaction times between 5 and 60 min. Pressures were high enough to keep the water in the liquid phase. At times, added sodium carbonate served as a catalyst. Bio-oil yields typically ranged from 35 to 65 wt %, and the bio-oil typically had a high N (~6 wt %) and O (~12 wt %) content. The heating value of the bio-oil was usually 35–50 MJ/kg. *Botryococcus braunii*, *Dunaliella tertiolecta*, *Spirulina*, and *Microcystis viridis* are among the species that have been liquefied hydrothermally. Significantly, an energy balance analysis showed that microalgae liquefaction can be a net energy producer.^{7,8}

Both gas and bio-oil products were analyzed for the hydrothermal processing of *M. viridis*.¹⁰ The highest oil yield (33 wt %) corresponded to an energy yield (defined as the ratio of the weight of C and H in bio-oil to the weight of C and H in the feedstock) of about 40%. The liquefied oil contained C17–C18 *n*-alkanes and polyaromatic hydrocarbons as the major constituents. The gas contained mostly CH₄ and CO₂, with only small amounts of H₂ and CO.

The liquefaction studies noted above were performed at subcritical temperatures (below 374 °C), and the desired

*To whom correspondence should be addressed. E-mail: psavage@umich.edu.

(1) Patil, V.; Tran, K.; Giselrod, H. R. *Int. J. Mol. Sci.* **2008**, *9*, 1188–1195.

(2) Miao, X.; Wu, Q. *J. Biotechnol.* **2004**, *110*, 85–93.

(3) Searchinger, T.; Heimlich, R.; Houghton, R. A.; Dong, F.; Elobeid, A.; Fabiosa, J.; Tokgoz, S.; Hayes, D.; Yu, T.-H. *Science* **2008**, *319*, 1238–1240.

(4) Dote, Y.; Sawayama, S.; Inoue, S.; Minowa, T.; Yokoyama, S. *Fuel* **1994**, *73*, 1855–1857.

(5) Sawayama, S.; Inoue, S.; Dote, Y.; Yokoyama, S. *Energy Convers. Manage.* **1995**, *36*, 729–731.

(6) Kishimoto, M.; Okakura, T.; Nagashima, H.; Minowa, T.; Yokoyama, S.; Yamaberi, K. *J. Ferment. Bioeng.* **1994**, *78*, 479–482.

(7) Minowa, T.; Yokoyama, S.; Kishimoto, M.; Okakura, T. *Fuel* **1995**, *74*, 1735–1738.

(8) Sawayama, S.; Minowa, T.; Yokoyama, S. *Biomass Bioenergy* **1999**, *17*, 33–39.

(9) Matsui, T.; Nishihara, A.; Ueda, C.; Ohtsuki, M.; Ikenaga, N.; Suzuki, T. *Fuel* **1997**, *76*, 1043–1048.

(10) Yang, Y. F.; Feng, C. P.; Inamori, Y.; Maekawa, T. *Resour., Conserv. Recycl.* **2004**, *43*, 21–33.

product was a liquid bio-oil. There have also been a few published studies that examined the gasification of algal biomass, often in supercritical water, for methane or syngas production.^{11–16} Nitrogen in the microalgae is reported to form ammonia during gasification. It can be recovered in the aqueous phase and then used as a source of nutrients for microalgae cultivation.^{11,12} High carbon gasification efficiencies ($C_{\text{gas}}/C_{\text{feed}}$) can be achieved via gasification in supercritical water at around 400 °C using ruthenium catalysts.^{14,15} A low microalgae concentration is typically required, and the low supercritical temperature results in a gas rich in methane and carbon dioxide. The nutrients, water, and carbon dioxide produced can be recycled.¹⁵ Chakinala et al.¹⁶ very recently investigated the supercritical water gasification of *Chlorella vulgaris*. The gas contained CO₂, CO, CH₄, H₂, and some C₂–C₃ compounds. Higher gasification efficiencies occurred at higher temperatures, lower algae concentrations, and longer residence times.

This brief review of the literature shows that hydrothermal liquefaction and supercritical water gasification of microalgae have previously been studied largely as two disparate topics. Of course, both gas and liquid products would be formed at all hydrothermal processing temperatures, whether sub- or supercritical. Therefore, rather than arbitrarily declaring subcritical processing to be “liquefaction” and supercritical processing to be “gasification”, we quantified and analyzed the oil and gas yields from hydrothermal processing over the temperature continuum from 200 to 500 °C. This paper is the first to report in detail yields and molecular compositions of both the oil and gas products from a systematic study of hydrothermal treatment over a broad temperature range. Our investigation focused on the analysis of the oil and gas phases. Thus, we did not retain or characterize the aqueous phase and solid residue formed during liquefaction. Additionally, this work is the first to explore the green alga *Nannochloropsis* sp. as a feedstock for biofuel production via thermochemical methods. *Nannochloropsis* sp. is a marine alga that can have a high oil (triglyceride) content.^{17–20} Moreover, Rodolfi et al.,²¹ who screened 30 microalgal strains for their lipid production potential, found that three members of the marine genus *Nannochloropsis* sp. demonstrated the best combination of both biomass productivity ($\sim 0.2 \text{ g L}^{-1} \text{ day}^{-1}$) and lipid content ($\sim 30 \text{ wt } \%$). These recent studies suggest that *Nannochloropsis* sp. is a good algal feedstock candidate for biofuel production.



Figure 1. Image of a batch stainless-steel reactor.

Table 1. Chemical Composition (wt % Dry Basis) of *Nannochloropsis* sp.

carbohydrates	12
proteins	52
lipids	28
elemental analysis	
C	43.3
H	6.0
O	25.1
N	6.4
S	0.5

Materials and Methods

We carried out all experiments in batch reactors assembled from 316 stainless-steel tubing and Swagelok fittings. We designed the reactors, pictured in Figure 1, to allow for the recovery and analysis of both the liquid- and gas-phase products in a single run. Each reactor had an internal volume of 35 mL and consisted of an 8 in. in length and $\frac{3}{4}$ in. in outer diameter tubing, with a wall thickness of 0.065 in. A cap was placed on one end, and the other end was fitted with an 8 in. in length and $\frac{1}{4}$ in. in outer diameter tubing, with a wall thickness of 0.035 in., which was connected to a high-pressure valve (HiP part 30-12HF2). Prior to their use in experiments, we loaded the reactors with water and treated them at 500 °C for 60 min to remove any residual organic material from the reactors and to expose the fresh metal walls to supercritical water. The reactors were then gradually cooled to ambient temperature, thoroughly washed with acetone, and air-dried. To facilitate experimental efficiency, we assembled five different reactors and used at least three of them simultaneously for parallel liquefaction experiments at each reaction temperature.

Nannochloropsis sp. was purchased as a paste (we determined experimentally that the paste contained 79 wt % water) from Reed Mariculture, Inc. (*Nannochloropsis* 3600) and was used as received. Table 1 provides the chemical composition of the alga (as provided by the supplier) and its elemental composition (as performed by Atlantic Microlab, Inc.). *Nannochloropsis* sp., a marine microalga, contains about 2–3 wt % of salt on a wet basis. The water was distilled and deionized prior to use. All other chemicals were purchased from Fischer Scientific in high purity and used as received. Argon and helium were obtained from Cryogenic Gases, with a purity of 99.998%.

We used an arbitrary microalgae paste loading of 4.27 g for all experiments ($\sim 0.90 \text{ g}$ on a dry basis). The amount of water loaded for experiments at subcritical temperatures ($T_c = 374 \text{ }^\circ\text{C}$) was such that the aqueous phase occupied 95% of the reactor volume at reaction conditions based on the density of pure water at the specific reaction temperature. Pressure can be determined from the saturated steam tables. We loaded between 1.3 and 12.3 g of water for experiments at supercritical temperatures, such that the pressure at the reaction temperature would be 35 000 kPa. After the reactors were loaded with microalgae paste and water, we connected the valve assembly to the reactor body and securely tightened it to seal the reactor. Residual air was removed from the sealed reactor by pressurizing it with helium, then venting it, and evacuating to an absolute pressure of 15 kPa. We conducted several helium flushing vacuum cycles to remove as much residual air as possible. Analysis via gas chromatography (GC) verified that the initial O₂ and N₂ present in the reactor were below detection limits. We then connected the purged reactors to a helium cylinder and pressurized them with helium at 69 kPa. This added helium served as a standard in the quantification of gas yields. After pressurization, the reactor valve was closed and the reactor assembly was then disconnected from the helium cylinder.

- (11) Minowa, T.; Sawayama, S. *Fuel* **1999**, *78*, 1213–1215.
- (12) Tsukahara, K.; Kimura, T.; Minowa, T.; Sawayama, S.; Yagishita, T.; Inoue, S.; Hanaoka, T.; Usui, Y.; Ogi, T. *J. Biosci. Bioeng.* **2001**, *91*, 311–313.
- (13) Hirano, A.; Hon-Nami, K.; Kunito, S.; Hada, M.; Ogushi, Y. *Catal. Today* **1998**, *45*, 399–404.
- (14) Stucki, S.; Vogel, F.; Ludwig, C.; Haiduc, A. G.; Brandenberger, M. *Energy Environ. Sci.* **2009**, *2*, 535–541.
- (15) Haiduc, A. G.; Brandenberger, M.; Suquet, S.; Vogel, F.; Bernier-Latmani, R.; Ludwig, C. *J. Appl. Phycol.* **2009**, *21*, 529–541.
- (16) Chakinala, A. G.; Brilman, D. W. F.; van Swaaij, W. P. M.; Kersten, S. R. A. *Ind. Eng. Chem. Res.* **2010**, *49*, 1113–1122.
- (17) Gouveia, L.; Oliveira, A. C. *J. Ind. Microbiol. Biotechnol.* **2009**, *36*, 269–274.
- (18) Chisti, Y. *Biotechnol. Adv.* **2007**, *25*, 294–306.
- (19) Sheehan, J.; Dunahay, T.; Benemann, J.; Roessler, P. A Look Back at the U.S. Department of Energy's Aquatic Species Program—Biodiesel from Algae. National Renewable Energy Laboratory, Golden, CO, 1998; NREL/TP-580-24190.
- (20) Suen, Y.; Hubbard, J. S.; Holzer, G.; Tornabene, T. G. *J. Phycol.* **1987**, *23*, 289–296.
- (21) Rodolfi, L.; Zittelli, G. C.; Bassi, N.; Padovani, G.; Biondi, N.; Bonini, G.; Tredici, M. R. *Biotechnol. Bioeng.* **2009**, *102*, 100–112.

After the reactors were loaded and pressurized with helium, we placed them in a fluidized sand bath (Techne SBL-2D) preheated to and maintained at the desired processing temperature by a temperature controller (Techne TC-8D). The sand bath was isothermal to within ± 1 and ± 5 °C for 200–400 and 450–500 °C, respectively. The body of each reactor was completely submerged vertically in the sand bath. We determined experimentally that the reactor contents reached the sand bath temperature within 3 min and then remained at that temperature thereafter. After the reaction time of 60 min had elapsed, we removed the reactors from the sand bath and immediately quenched them in a cool water bath. The reactors were further cooled in a refrigerator for 30 min. We then removed the reactors from the refrigerator and placed them in ambient conditions for at least 1 h to allow the liquid–gas system to reach equilibrium. With the exception of the experiment conducted at 500 °C, we performed 5–6 runs at each temperature to determine the uncertainties in the experimental results. Results reported herein represent mean values, and uncertainties are standard deviations.

The gaseous products were analyzed with an Agilent Technologies model 6890N gas chromatograph (GC) equipped with a thermal conductivity detector (TCD). A 15 ft \times $\frac{1}{8}$ in. inner diameter stainless-steel column, packed with 60 \times 80 mesh Carboxen 1000 (Supleco), separated each component in the mixture. Argon (15 mL/min) served as the carrier gas for the analysis.

The reactor was connected to the GC gas-sampling valve, and the gases in the reactor flowed into the sample loop. The gas sample was sent to the column via a Valco switching valve, which was automated with an air actuator. After the switching valve was closed, the reactor valve was also closed. The temperature of the column was initially held at 35 °C for 5 min and then increased to 225 °C at a rate of 20 °C/min. The final temperature was held for 15 min, giving a total runtime of 35 min. Gas standards were purchased from Air Liquide Specialty Gases and analyzed to generate a calibration curve relating the mole fraction, y_i , and peak area for each component. The molar amount, n_i , of each component was subsequently calculated from

$$n_i = (y_i/y_{\text{He}})n_{\text{He}} \quad (1)$$

We used the ideal gas law to determine the moles of helium in the reactor. Two consecutive analyses of the gas mixture were performed for each reactor, and we used the average values to calculate the gas yields.

After analyzing the gas fraction, we opened the reactors to recover the liquid fraction. Equal volumes, 15 mL each, of dichloromethane and water were added, and the reactor was then capped and shaken by hand. The purpose of adding the water was to remove any residual water-soluble components and to facilitate recovering the organic phase containing the bio-oil. We then transferred the reactor contents to a glass separatory funnel. This reactor washing was repeated 2 more times to ensure that all of the reactor contents were recovered and transferred to the separatory funnel. After the aqueous and organic phases had separated, we withdrew the organic phase for further analysis. The organic phase contained a flaky solid residue, which was separated via centrifugation for 5 min at a rate of 400 relative centrifugal forces (rcf). We then carefully transferred the organic phase to a round-bottom flask via a pipet. The dichloromethane solvent was evaporated under a vacuum of about 11 kPa at 35 °C for 5 min. The flask was then quickly capped and weighed to determine the mass that it contained. The material remaining in the flask is the crude bio-oil plus residual dichloromethane. To estimate this residual solvent amount, we performed a control experiment, wherein we treated a flask containing pure dichloromethane alone to this evaporation procedure. The mass of residual solvent (0.08 g) in the control experiment was subtracted from the sample masses to estimate the mass of the crude bio-oil produced in each experiment. The bio-oil yield was calculated as its mass divided by the mass of microalgae loaded to the reactor

Table 2. Bio-oil Yields and Heating Values

temperature (°C)	oil yield (wt %)	heating value (MJ/kg)
25	22 \pm 3	39
200	27 \pm 8	39
250	38 \pm 2	38
300	32 \pm 6	38
350	43 \pm 2	39
400	40 \pm 3	39
450	38 \pm 4	39
500	16	37

on a dry basis. A portion of this bio-oil was reserved for elemental analysis by Atlantic Microlab, Inc. Of the 5–6 runs conducted at each temperature, only one sample from one run at each temperature was analyzed for C, H, O, N, and S contents. Duplicate analysis of each element was conducted for each sample. Results reported herein are the mean values.

After being weighed, the bio-oil was redissolved in about 10 mL of dichloromethane and stored in a refrigerator while awaiting GC analysis. We used an Agilent Technologies 6890N GC equipped with an autosampler, autoinjector, and mass spectrometric detector to qualitatively analyze the bio-oil. An Agilent J&W DB-5HT nonpolar capillary column (30 m length, 0.250 mm inner diameter, and 0.10 μ m film thickness) separated the constituents. A volume of 1.0 μ L was injected for each sample. The inlet split ratio was 5:1. The column was initially held at 80 °C for 2 min. The temperature then increased 3 °C/min to 300 °C, which was then held for 10 min. Helium served as the carrier gas (1 mL/min). A Wiley mass spectral library was used for compound identification.

Results and Discussion

This section presents results from hydrothermal processing experiments conducted at 200–500 °C in 50 °C increments. We report yields, elemental and molecular compositions, and energy content for both the gaseous products and the bio-oil. The influence of the temperature on these quantities is discussed in detail.

Control Experiment. Before presenting results from hydrothermal processing at elevated temperatures, we first report the results from a control experiment conducted at room temperature (about 25 °C). A reactor loaded with 4.27 g of *Nannochloropsis* sp. paste and about 15 g of water was placed in the sand bath for 60 min at ambient temperature. Then, the contents of the reactor were subjected to the same product recovery procedure used to remove the bio-oil post-reaction. The “bio-oil” remaining after evaporating the dichloromethane appeared as a green film on the round-bottom flask. Its yield was 22 wt %. Gas chromatography–mass spectrometry (GC–MS) analysis revealed that the five most abundant compounds were palmitoleic and palmitic acids, heptadecane, neophyadiene, and cholesterol. These compounds likely originated from the lipid portion of the microalgae, because lipids are generally hydrophobic but readily miscible in an organic solvent at ambient conditions. Proteins and carbohydrates are more hydrophilic. We suspect that the amount of material represented by the total ion chromatogram is just a small fraction of the total and that the green film contained significant amounts of high-molecular-weight material that would not elute from the GC column.

We are not aware of any similar control experiments having previously been reported in the literature. The present results, however, which reveal a 22 wt % “oil” yield at room temperature, indicate that the solvent, which is added with the intention of simply dissolving crude bio-oil produced by hydrothermal liquefaction, may also extract compounds

Table 3. Elemental Composition (wt %) of Bio-oil and *Nannochloropsis* sp. Feedstock

temperature (°C)	C	H	O	N	S	H/C	O/C	N/C
dry algae	43.3 ± 0.09	6.0 ± 0.01	25.1 ± 0.08	6.4 ± 0.02	0.53 ± 0.07	1.65	0.43	0.13
25	76.1 ± 0.03	10.7 ± 0.01	12.2 ± 0.02	0.73 ± 0.01		1.68	0.12	0.008
200	74.6 ± 0.13	10.8 ± 0.11	11.8 ± 0.06	2.4 ± 0.04	0.44 ± 0.12	1.73	0.12	0.027
250	75.0 ± 0.04	10.2 ± 0.09	10.3 ± 0.04	4.1 ± 0.01	0.55 ± 0.06	1.63	0.10	0.047
300	75.2 ± 0.05	10.3 ± 0.02	9.8 ± 0.00	4.3 ± 0.02	0.79 ± 0.05	1.64	0.097	0.049
350	76.0 ± 0.08	10.3 ± 0.00	9.0 ± 0.08	3.9 ± 0.02	0.89 ± 0.04	1.63	0.089	0.044
400	76.7 ± 0.01	10.3 ± 0.01	8.7 ± 0.09	3.6 ± 0.04	0.91 ± 0.08	1.61	0.085	0.040
450	76.8 ± 0.04	10.2 ± 0.03	7.7 ± 0.01	4.3 ± 0.01	1.0 ± 0.08	1.59	0.075	0.047
500	81.2 ± 0.11	7.1 ± 0.02	5.3 ± 0.07	4.4 ± 0.01	0.48 ± 0.03	1.04	0.049	0.047
crude oil	83.0–87.0	10.0–14.0	0.1–1.5	0.1–2.0	0.5–6.0			

from the algal biomass that were not produced or liberated via hydrothermal processing. Again, we believe that the amount of any true oil-range molecules produced in this control experiment is quite low.

Bio-oil Analysis. Table 2 displays the yield and heating values of the bio-oil produced from liquefaction at each temperature investigated. The oil yields that we report should probably be viewed as lower bounds, because the bio-oil that we recover is missing the lighter ends that would have been present. These lighter, more volatile molecules evaporate along with the dichloromethane solvent as we recover the oil.

The oil yield initially increased with the temperature, reaching 43 wt % at 350 °C. Because the lipid content of the original microalgae is only 28 wt %, the bio-oil clearly contains constituents that originate from the protein and carbohydrate components within the cell. The oil yield decreased modestly from this maximum value at 400 and 450 °C, but it was nearly halved at 500 °C. At these higher temperatures (supercritical conditions), oil-range molecules likely react to form both lighter, more volatile compounds that are not captured in the oil fraction and heavier higher molecular-weight compounds that remain in the solid residue. This scenario is consistent with the gas yields increasing with the temperature and with the appearance of condensed aromatic compounds in the oil at 500 °C. These results will be presented more completely in a subsequent section.

We used the Dulong formula to estimate the heating value of the bio-oils

$$\text{heating value (MJ/kg)} = 0.338C + 1.428(H - O/8) + 0.095S \quad (2)$$

where *C*, *H*, *O*, and *S* are the weight percentages of carbon, hydrogen, oxygen, and sulfur, respectively (see Table 3). The heating value was around 39 MJ kg^{−1} for all of the bio-oils, except that produced at 500 °C, which was slightly lower. These heating values are slightly lower than that of petroleum crude oil (43 MJ kg^{−1}) but significantly higher than that of the dry microalgal feedstock (~19 MJ kg^{−1}).

Table 3 shows the elemental composition of the bio-oil produced from liquefaction at each temperature investigated. Similar information about the dry microalgae feedstock, the “oil” from the control experiment, and petroleum crude oil is provided for comparison. The elemental analysis showed that the carbon content of the oil always exceeded that of the dried raw algae (43.3 wt %). The carbon content in the biocrude increased from 74.6 wt % at 200 °C to 81.2 wt % at 500 °C. The hydrogen content always exceeded 10 wt %, except at 500 °C, where it was 7.1 wt %. The oxygen content in the oil decreased steadily with an increasing temperature. Moreover, the oxygen content, although ranging from 5.3 to 11.8 wt %, was always much lower than that of the algal

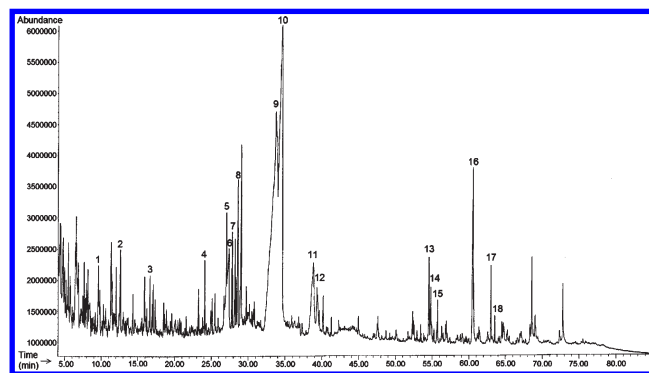


Figure 2. Total ion chromatogram for bio-oil obtained from liquefaction at 350 °C.

biomass (25.1 wt %). The bio-oil also contained significant quantities of N and S heteroatoms. The sulfur content increased with the temperature, except at 500 °C, where it was lower. The nitrogen content showed no clear trend with the temperature, but the nitrogen content of the oil was always less than that of the original algal biomass. The elemental analysis results clearly show that hydrothermal liquefaction produces a bio-oil that is enriched in carbon and hydrogen and has reduced levels of N and O compared to the original algal biomass feedstock. This elemental composition is comparable to that of petroleum crude oil, with the exception of the oxygen and nitrogen content being higher in the bio-oil. Thus, upgrading of the liquefied microalgae, especially deoxygenation and denitrogenation, is necessary.

Another way to interpret the elemental composition data is in terms of atomic ratios (e.g., H/C and O/C). The H/C ratio of the dry algal biomass is 1.65, and the bio-oils produced at subcritical temperatures have similar values. These values compare favorably to H/C ratios in petroleum crude oils. The H/C ratio drops to 1.04 at 500 °C, suggesting a more aromatic nature for this product. The N/C ratio is between 0.04 and 0.05 for the bio-oils produced at 250 °C and above. This ratio is about a third of that for the original algal biomass feedstock. The O/C ratio in the bio-oil decreases steadily with the liquefaction temperature from 0.12 to 0.049. The O/C ratio for the original algae is 0.43; therefore, liquefaction performs a significant extent of deoxygenation. Of course, additional deoxygenation is required to produce a fungible transportation fuel.

Elemental analysis provides information about the overall composition of the bio-oil, but it does not provide any molecular-level detail. Therefore, we used GC–MS to obtain information about the amounts and identities of specific molecules in the bio-oil. Figure 2 displays a total ion chromatogram for the bio-oil produced from liquefaction at 350 °C, the temperature at which the maximum oil yield was obtained.

Table 4. Major Identified Molecular Products from Liquefaction at 350 °C

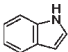
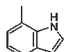


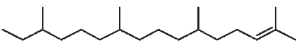
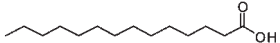
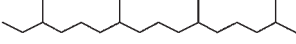
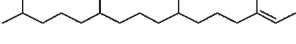
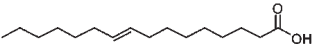
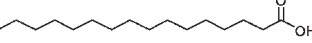
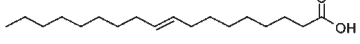
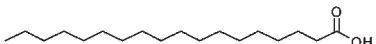
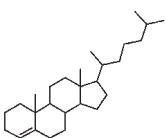
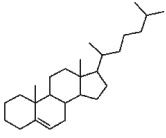
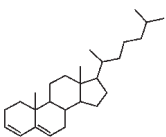
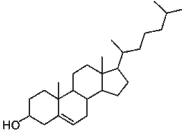
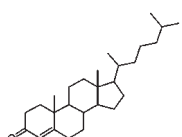
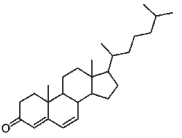
Peak ID in Fig. 3	Compound	Structure	Peak Area %	R.T. (min)
1	Indole		1.23	9.60
2	Methylindole		1.25	12.61
3	1-Pentadecene		0.47	16.64
4	Heptadecane		0.54	24.09
5	2-Phytene Isomer		2.03	27.06
6	Myristic Acid		2.62	27.39
7	Phytane		0.98	27.81
8	2-Phytene Isomer		2.77	28.63
9	Palmitoleic Acid		24.02	33.75
10	Palmitic Acid		18.61	34.59
11	Oleic Acid		3.61	38.83
12	Stearic Acid		0.56	39.31
13	Cholest-4-ene		0.92	54.56
14	Cholest-5-ene		0.49	54.80
15	Cholesta-3,5-diene		0.58	55.75
16	Cholesterol		2.73	60.55
17	Cholest-4-en-3-one		0.79	63.01
18	Cholest-4,6-diene-3-one		0.23	63.52

Table 5. Fatty Acid Composition of *Nannochloropsis* sp.

common name	shorthand designation	weight %
myristic acid	C14:0	5.31
myristoleic acid	C14:1	0.92
pentadecylic acid	C15:0	0.31
pentadecenoic acid	C15:1	0.26
palmitic acid	C16:0	19.75
palmitoleic acid	C16:1	29.52
margaric acid	C17:0	0.33
heptadecenoic acid	C17:1	0.45
stearic acid	C18:0	0.42
oleic acid	C18:1	3.37
linoleic acid	C18:2	2.10
nonadecylic acid	C19:0	0.42
eicosatrienoic acid	C20:3	0.16
arachidonic acid	C20:4	5.12
eicosapentaenoic acid	C20:5	29.81
behenic acid	C22:0	0.49
erucic acid	C22:1	0.27
brassic acid	C22:2	0.12

Nearly 90 different compounds were detected. Keep in mind, however, that the bio-oil likely contained additional compounds that do not appear in the chromatogram. Lighter products were lost during solvent evaporation or were masked by the solvent during analysis, and very heavy compounds are not likely to elute from the GC column and be detected. We used matches with mass spectra of known compounds stored in the computer library and manual inspection of MS fragmentation patterns for each peak to identify 39 individual molecular components of the biocrude. These components represent more than 70% of the total peak area. Table 4 lists the identities and relative amounts of selected molecular species that correspond to the labeled peaks in Figure 2.

Table 4 includes two heterocyclic N-containing compounds, indole and methyl indole. The pyrrole moiety in indole is also present in biomacromolecules, including chlorophyll, which is abundant in algal biomass. Thus, indole formation may be due to the hydrolysis of chlorophyll into smaller fragments. Two other major constituents of the bio-oil are phytane and phytene. Similar to indole, both compounds are associated with chlorophyll, which contains a chlorine ring with a phytol and other side chains. It is possible that phytol formed from the hydrolysis of chlorophyll and then underwent further reactions. We detected phytol only at the lower liquefaction temperatures of 200 and 250 °C, whereas phytane and phytene appeared at reaction temperatures of 300, 350, 400, and 450 °C. Phytane can be produced from the hydrogenolysis of phytol.²²

Table 4 also includes five free fatty acids, myristic, palmitoleic, palmitic, oleic, and stearic acids. These products were also observed in the bio-oils produced at other temperatures. These fatty acids likely arise from hydrolysis of triacylglycerols present in the *Nannochloropsis* sp., which is about 28% lipids. We characterized the fatty acid distribution in dry *Nannochloropsis* sp. via hexane extraction of the lipids, and Table 5 shows the results. The major fatty acids are eicosapentaenoic acid (EPA) (C20:5), palmitoleic acid (C16:1), palmitic acid (C16:0), myristic acid (C14:0), and arachidonic acid (C20:4), with lesser amounts of oleic acid (C18:1) and linoleic acid (C18:2). These results are consistent with other published data.²³ This triacylglycerol profile for *Nannochloropsis* sp. shows that the five fatty acids observed in the bio-oil also account for nearly 60% of the fatty acid content in the

Table 6. Minor Identified Molecular Products from Liquefaction at 350 °C

compound name	peak area (%)	retention time (RT) (min)
C ₈ H ₁₂ O cycloalkene ketone	0.86	4.39
4-methylphenol	0.38	4.46
1-ethyl-2-pyrrolidinone	1.01	4.71
trimethyltetralin	0.50	11.49
dimethylnaphthalene	0.11	13.54
dimethylindole	0.25	16.22
pentadecane	0.24	16.94
3-hydroxy-trimethyltetralin	0.29	18.90
cycloalkane	0.44	23.24
1-heptadecene	0.13	23.79
3-eicosene	0.50	26.71
nonadecane	0.19	30.73
palmitic acid amide	0.49	39.40
C ₂₀₊ alkane	0.18	47.62
C ₂₀₊ alkene	0.24	52.34
C ₂₀₊ alkane	0.10	52.46
cyclononacosane	0.14	56.84
nonacosane	0.14	56.94
cholestanol	0.52	60.64
fucosterol	0.19	64.50
1,30-triacontanediol	0.13	64.66

dry microalga. Of course, there may be other pathways to fatty acids during hydrothermal liquefaction because palmitic acid was reported to be a constituent of the bio-oil from sawdust, which contains no triglycerides.²⁴ The algal bio-oils also contained a considerable amount of cholesterol and related compounds. Similar to triacylglycerols, cholesterol would likely arise from the lipid fraction of the algal biomass.

Heptadecane was observed at all liquefaction temperatures, with the exception of 500 °C. A pathway for its formation is decarboxylation of the corresponding fatty acid (i.e., stearic acid). This reaction is very slow in pure high-temperature water, but it is possible that the minerals present in the algal biomass serve to catalyze decarboxylation, especially at the higher temperatures. There may also be a nonhydrothermal source of heptadecane, however, because it was also present in the “oil” from the control experiment. Additional evidence pointing to the existence of other pathways for alkanes is the presence of long-chain alkanes in bio-oils from the liquefaction of corn stalks²⁵ and sawdust,²⁶ which do not contain appreciable amounts of fatty acids.

Table 6 lists the remaining 21 species that we identified in the bio-oil produced at 350 °C. Most of these peaks were too small to label in Figure 2. Phenol and its alkylated derivatives, including 4-methylphenol, were observed at reaction temperatures of 300 °C and greater. Phenol might be a product from the carbohydrate portion of the algal biomass, because hydrothermal treatment of cellulose and glucose^{27–29} produced phenols. Table 6 shows the presence of the additional N-containing compounds, 1-ethyl-2-pyrrolidinone, dimethylindole, and palmitic acid amide. The two heterocyclic N compounds include a pyrrolic moiety, which is also characteristic of chlorophyll. A possible pathway for the formation of palmitic acid amide is the reaction of palmitic acid with

(24) Karagoz, S.; Bhaskar, T.; Muto, A.; Sakata, Y.; Uddin, M. A. *Energy Fuels* **2004**, *18*, 234–241.

(25) Wang, C.; Pan, J.; Li, J.; Yang, Z. *Bioresour. Technol.* **2008**, *99*, 2778–2786.

(26) Xu, C.; Lad, N. *Energy Fuels* **2008**, *22*, 635–642.

(27) Williams, P. T.; Onwudili, J. *Ind. Eng. Chem. Res.* **2005**, *44*, 8739–8749.

(28) Nelson, D. A.; Molton, P. M.; Russell, J. A.; Hallen, R. T. *Ind. Eng. Chem. Prod. Res. Dev.* **1984**, *23*, 471–475.

(29) Sinag, A.; Kruse, A.; Schwarzkopf, V. *Ind. Eng. Chem. Res.* **2003**, *42*, 3516–3521.

(22) Huang, K.; Armstrong, D. W. *Org. Geochem.* **2009**, *40*, 283–286.

(23) Sukenik, A.; Carmeli, Y. *J. Phycol.* **1989**, *25*, 686–692.

Table 7. Effect of the Processing Temperature on the Gas Composition

temperature (°C)	composition (mol %)					
	H ₂	CH ₄	CO ₂	CO	N ₂	C ₂ H ₄
200	0.39 ± 0.14	0.05 ± 0.02	88.0 ± 4.5		11.5 ± 4.3	
250	0.42 ± 0.18	0.25 ± 0.06	97.0 ± 0.9		2.3 ± 0.6	
300	5.1 ± 0.9	0.8 ± 0.04	91.5 ± 2.0		1.0 ± 0.3	0.64 ± 0.3
350	29.7 ± 1.9	1.9 ± 0.1	66.2 ± 1.9		0.43 ± 0.06	1.2 ± 0.07
400	38.6 ± 3.3	3.0 ± 0.5	56.2 ± 4.1			0.96 ± 0.07
450	35.1 ± 1.5	6.1 ± 1.3	54.5 ± 2.8	0.43 ± 0.14		0.92 ± 0.06
500	19.3 ± 0.4	32.6 ± 0.3	36.0 ± 0.9	0.28 ± 0.01		0.53 ± 0.01

Table 8. Effect of the Processing Temperature on Gas Yields and Heating Values

temperature (°C)	C (%)	H (%)	O (%)	total yield (mmol/g)	heating value (MJ/kg)
200	0.23 ± 0.06	0.001 ± 0.001	1.1 ± 0.3	0.10 ± 0.02	0.03
250	1.3 ± 0.2	0.015 ± 0.007	5.7 ± 1.0	0.46 ± 0.08	0.10
300	2.5 ± 0.5	0.32 ± 0.10	10.9 ± 2.5	0.93 ± 0.21	1.1
350	3.5 ± 0.3	2.2 ± 0.1	14.8 ± 1.4	1.8 ± 0.1	4.2
400	6.1 ± 0.3	5.8 ± 0.9	24.5 ± 1.4	3.4 ± 0.2	6.4
450	8.6 ± 2.2	8.9 ± 2.7	31.0 ± 6.8	4.5 ± 1.1	8.2
500	42.2 ± 1.3	65.9 ± 1.1	75.7 ± 3.8	16.4 ± 0.4	21.1

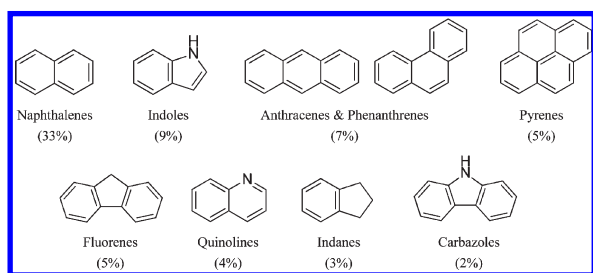


Figure 3. PAHs in the bio-oil produced at 500 °C.

ammonia. Palmitic acid was present in large amounts in the bio-oil, and we expect ammonia to be abundant in the liquefaction mixture as well. 3-Eicosene, a C₂₀ alkene, is a product that might have arisen from the lipid portion of the algal biomass, which is about one-third C₂₀₊ fatty acid. Long-chain alkanes and alkenes, including a substantial amount of C₂₀₊ hydrocarbons, were observed in the bio-oil. Several cycloalkanes were also found in the bio-oils at reaction temperatures above 350 °C.

Polycyclic aromatic hydrocarbons (PAHs) and their alkylated derivatives were found in all bio-oils produced at 300 °C and above. These compounds were the dominant species in the oil produced at 500 °C. Figure 3 illustrates the PAHs prevalent at 500 °C, along with their percentages of the total chromatogram peak area. In addition, about 3% of the total peak area corresponded to triphenylene, benzopyrene, and benzoperylene. Many compounds, including plant sterols, yield PAHs under pyrolytic conditions.³⁰ Although the formation of PAHs has been documented from a variety of sources, the reaction mechanisms and intermediates remain unclear.

Gas Fraction Analysis. Table 7 shows the identities and molar concentrations of different permanent gas products from hydrothermal treatment of microalgae at different temperatures. The major combustible products were H₂ and CH₄, with smaller amounts of C₂H₄ and C₂H₆. Very little or no CO is present across the temperature range, which

suggests that any CO formed was consumed, perhaps in the water–gas shift and/or methanation reactions.^{31,32}

The temperature had a significant influence on the product gas composition. The gas became richer in hydrocarbons (CH₄ and C₂) as the hydrothermal processing temperature increased. The mole fractions of CO₂ and N₂, on the other hand, decreased as the temperature increased. N₂ must be formed from nitrogen atoms in the microalgae because we removed the residual air from the reactor prior to hydrothermal treatment. The H₂ mole fraction reached a maximum of about 39% in the gases produced at 400 °C. These results show that the gas composition is a strong function of the hydrothermal processing temperature.

The temperature also had a significant effect on the gas yields and heating value, shown in Table 8. The C, H, and O yields were calculated as the percentages of the number of C, H, or O atoms in the initial dry microalgae that appear in the product gases. The highest yields of C, H, and O are 42, 66, and 76%, respectively, at 500 °C. It was also at this temperature that the bio-oil yield decreased substantially. Thus, it seems that, at this high temperature, molecules that were originally in the oil were cracked to form smaller, lighter compounds that eventually formed permanent gases. Heat of combustion data for each gas-phase component were used to calculate the heating value of the total gas product at each reaction temperature. The energy content of the gas increased with the temperature, reaching a maximum value of about 21 MJ kg^{−1} at 500 °C.

As the temperature increased, the amounts of all of the gas constituents (except CO and N₂) also increased. If the gas yields are proportional to the average rate of gas formation during the 60 min reaction, we can calculate apparent activation energies for the formation of each gas. Finding similar activation energies for different gas species would suggest a common reaction path for their formation. We calculated the activation energies for H₂ and CO₂ to be 99 ± 5 and 38 ± 3 kJ/mol, respectively. These very different values suggest that the reaction(s) that primarily increase the yields of H₂ are not the same as those that increase the yields of CO₂. Therefore, it appears that neither water–gas shift nor steam reforming is the sole dominant pathway for these two products. A similar analysis of activation energies for gas formation during supercritical water gasification (SCWG) of lignin and cellulose led to the same conclusion for those

(30) Bager, G. M.; Donnelly, J. K.; Spotswood, T. M. *Aust. J. Chem.* **1965**, *18*, 1249–1266.

(31) Rice, S. F.; Steeper, R. R.; Aiken, J. D. *J. Phys. Chem. A* **1998**, *102*, 2673–2678.

(32) Sato, T.; Kurosawa, S.; Smith, R. L.; Adschiri, T.; Arai, K. *J. Supercrit. Fluids* **2004**, *29*, 113–119.

Table 9. Atom (wt %) and Energy Recoveries in Gas and Bio-oil Products

temperature (°C)	C		H		O		N		S	energy recovery
	total	oil	total	oil	total	oil	total	oil	total	
200	47 ± 9	46 ± 9	49 ± 9	49 ± 9	14 ± 4	13 ± 4	10 ± 3	9 ± 3	22 ± 7	0.55
250	67 ± 3	66 ± 3	65 ± 3	65 ± 3	21 ± 1	16 ± 1	25 ± 1	24 ± 1	39 ± 2	0.77
300	58 ± 8	56 ± 8	56 ± 9	55 ± 9	23 ± 3	12 ± 2	22 ± 4	21 ± 4	48 ± 9	0.67
350	78 ± 4	75 ± 4	76 ± 4	74 ± 4	30 ± 1	15 ± 1	26 ± 1	26 ± 1	71 ± 4	0.90
400	77 ± 5	71 ± 5	75 ± 6	70 ± 5	38 ± 2	14 ± 1	22 ± 2	22 ± 2	69 ± 5	0.87
450	76 ± 6	67 ± 7	74 ± 6	65 ± 6	43 ± 7	12 ± 1	25 ± 2	25 ± 2	73 ± 7	0.85
500	72 ± 1	30	85 ± 1	19	79 ± 4	3	11	11	15	0.78

feedstocks; therefore, this conclusion might be generally true for uncatalyzed SCWG.³³ The activation energies for CH₄, C₂H₆, and C₂H₄ were 108 ± 3, 105 ± 6, and 67 ± 8 kJ/mol, respectively. At the lower temperatures where N₂ was detected (200–350 °C), its activation energy for formation was 5 ± 1 kJ/mol.

Having presented detailed results for both the bio-oil and gas-phase products, we now combine these analyses to determine total yields of the different elements in the fuel products formed at each temperature and to determine the overall energy recovery. Table 9 presents the results. The C, H, and O recoveries generally increased with the temperature. At the near- and supercritical temperatures, the combined bio-oil and gas contained about 80% as much carbon and hydrogen as the original microalgae on a dry basis. The bio-oil fraction always contained more of the carbon than the gas fraction, but the relative contributions from both the gas and oil were nearly equal at 500 °C. We speculate that, if even modestly higher temperatures were examined, the gas fraction would contain more of the carbon than the oil. The H and O atom recoveries are both less than 100%, but this outcome does not rule out the possibility of water molecules having been active participants in the chemistry and H and O atoms from water being incorporated into the oil and gas products. Both gas-phase reactions (e.g., water–gas shift and steam reforming) and liquefaction reactions (e.g., hydrolysis) are expected to involve water as a reactant. The N recovery was generally around 25%, except at 200 and 500 °C where it was about half as much. The S recovery increased with the temperature up to 450 °C, but the S content of the fuels at 500 °C was much lower. It is likely that the lower S content at 500 °C was due to its partitioning into the dichloromethane-insoluble solids or its appearance as H₂S, a gas for which we did not analyze. The energy recovery, defined as the combined heating values of the oil and gas products divided by the heating value of the original microalgae (dry basis) loaded to the reactor, was near unity. This result suggests that the hydrothermal liquefaction of *Nannochloropsis* sp. leads to fuel products that have as much stored chemical energy as the dry microalgal feedstock. Note too that the energy content in the product could, in principle, exceed that of the dry biomass because of the participation of water molecules in various

reaction pathways during hydrothermal processing. Taken collectively, the results in Table 9 show that hydrothermal processing of this microalga can produce liquid and gaseous fuels that contain about 80% of the carbon and hydrogen contents and 90% of the energy content of the feedstock but much lower percentages of the O and N atoms.

Conclusions

A crude bio-oil with a H/C ratio resembling that of petroleum crude oil can be produced from *Nannochloropsis* sp. via hydrothermal liquefaction at 250–450 °C. At the maximum yield, the bio-oil contained 75% of the carbon in the microalgae feedstock but only 15% of the oxygen and about 25% of the nitrogen. The oil and gas products produced from liquefaction contain roughly the same amount of chemical energy as the microalga feedstock.

We measured a 22 wt % yield of “bio-oil” from algae paste that never experienced hydrothermal reaction conditions when it was treated to the product recovery method used in the experiments. This material was simply extracted from the *Nannochloropsis* sp. by the added dichloromethane. Therefore, the prevalent operational definition of bio-oil from microalgae (i.e., post-reaction material that partitions into dichloromethane or some other light solvent) may be inadequate. Better methods need to be developed for recovering the true bio-oil fraction formed via liquefaction.

The nature of the molecules in the bio-oil changed as the liquefaction temperature increased. Lower temperatures produced fatty acids, alkanes, alkenes, sterol-related compounds, and heterocyclic N-containing compounds. The higher temperatures produced more PAHs, and at 500 °C, PAHs were nearly the exclusive products observed in the total ion chromatograms. Likewise, the composition of the gas changed with the temperature. As the temperature increased, the total gas yield and the mole fractions of hydrocarbons (CH₄ and C₂) in the gas increased.

Acknowledgment. We thank Robert Levine for experimental assistance. T. M. Brown gratefully acknowledges the National Science Foundation (NSF) Alliance for Graduate Education and the Professoriate (AGEP) Fellowship Program for financial support, and we acknowledge financial support from the University of Michigan College of Engineering and NSF (CBET-0755617 and EFRI-0937992).

(33) Resende, F. L. P.; Savage, P. E. *Energy Fuels* 2009, 23, 6213–6221.